

# SUPPORTING INFORMATION

## ESI-MS Study of the Interaction of Potential Oxidovanadium(IV) Drugs and Amavadin with Model Proteins

*Valeria Ugone,<sup>§</sup> Daniele Sanna,<sup>†</sup> Giuseppe Sciortino,<sup>§,#</sup> Debbie C. Crans,<sup>¶</sup> and  
Eugenio Garribba<sup>\*,§</sup>*

<sup>§</sup> Dipartimento di Chimica e Farmacia, Università di Sassari, Via Vienna 2, I-07100 Sassari, Italy

<sup>†</sup> Istituto CNR di Chimica Biomolecolare, Trav. La Crucca 3, I-07040 Sassari, Italy

<sup>#</sup> Departament de Química, Universitat Autònoma de Barcelona, 08193 Cerdanyola del Vallés,  
Barcelona, Spain

<sup>¶</sup> Department of Chemistry, Colorado State University, 1301 Center Avenue, Fort Collins,  
Colorado, USA

Corresponding author. E-mail: garribba@uniss.it (E.G.).

**Table S1.** Identified species in the ESI-MS spectra of the system containing  $[V^{IV}O(pic)_2(H_2O)]$ .

Ion	Composition	Experimental m/z <sup>a</sup>	Calculated m/z <sup>a</sup>	Error (ppm) <sup>b</sup>
$[Hpic+H]^+$	$C_6H_6NO_2$	124.03952	124.03930	-1.8
$[Hpic+Na]^+$	$C_5H_6NO_2Na$	146.02125	146.02125	0.0
$[pic]^-$	$C_6H_4NO_2$	122.02360	122.02475	9.4
$[V^{IV}O(pic)_2+H]^+$	$C_{12}H_9N_2O_5V$	311.99453	311.99456	0.1
$[V^{IV}O(pic)_2+Na]^+$	$C_{12}H_8N_2O_5VNa$	333.97647	333.97651	0.1
$[V^{IV}O(pic)_2(OH)]^-$	$C_{12}H_8N_2O_6V$	326.98299	326.98275	-0.7
$[V^VO_2(pic)_2]^-$	$C_{12}H_9N_2O_6V$	327.99083	327.99057	-0.8

<sup>a</sup> Experimental and calculated m/z values refer to the peak representative of the monoisotopic mass.

<sup>b</sup> Error in ppm respect to the experimental value, calculated as:  $10^6 \times \{[| \text{Calculated (m/z)} - \text{Experimental (m/z)} |] / \text{Calculated (m/z)}\}$ .

**Table S2.** Identified species in the ESI-MS spectra of the system containing  $[V^{IV}O(ma)_2]$ .

Ion	Composition	Experimental m/z <sup>a</sup>	Calculated m/z <sup>a</sup>	Error (ppm) <sup>b</sup>
$[Hma+H]^+$	$C_6H_7O_3$	127.03908	127.03897	-0.9
$[ma]^-$	$C_6H_5O_3$	125.0234	125.0244	8.0
$[V^{IV}O(ma)_2+H]^+$	$C_{12}H_{11}O_7V$	317.99328	317.99389	1.9
$[V^VO_2(ma)_2]^-$	$C_{12}H_{10}O_8V$	332.98251	332.98208	-1.3

<sup>a</sup> Experimental and calculated m/z values refer to the peak representative of the monoisotopic mass.

<sup>b</sup> Error in ppm respect to the experimental value, calculated as:  $10^6 \times \{[| \text{Calculated (m/z)} - \text{Experimental (m/z)} |] / \text{Calculated (m/z)}\}$ .

**Table S3.** Identified species in the ESI-MS spectra of the system containing [V<sup>IV</sup>O(dhp)<sub>2</sub>].

Ion	Composition	Experimental m/z <sup>a</sup>	Calculated m/z <sup>a</sup>	Error (ppm) <sup>b</sup>
[V <sup>IV</sup> O(dhp) <sub>2</sub> +H] <sup>+</sup>	C <sub>14</sub> H <sub>17</sub> N <sub>2</sub> O <sub>5</sub> V	344.05698	344.05716	0.5
[V <sup>IV</sup> O(dhp) <sub>2</sub> +Na] <sup>+</sup>	C <sub>14</sub> H <sub>16</sub> N <sub>2</sub> O <sub>5</sub> VNa	366.03958	366.03911	-1.3

<sup>a</sup> Experimental and calculated m/z values refer to the peak representative of the monoisotopic mass.

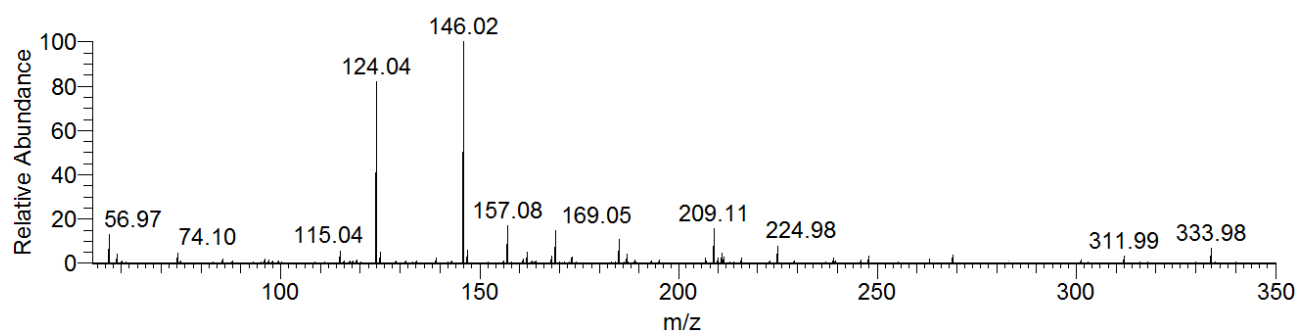
<sup>b</sup> Error in ppm respect to the experimental value, calculated as:  $10^6 \times \{ [| \text{Calculated (m/z)} - \text{Experimental (m/z)} |] / \text{Calculated (m/z)} \}$ .

**Table S4.** Identified species in the ESI-MS spectra of the system containing  $[V^{IV}O(acac)_2]$ .

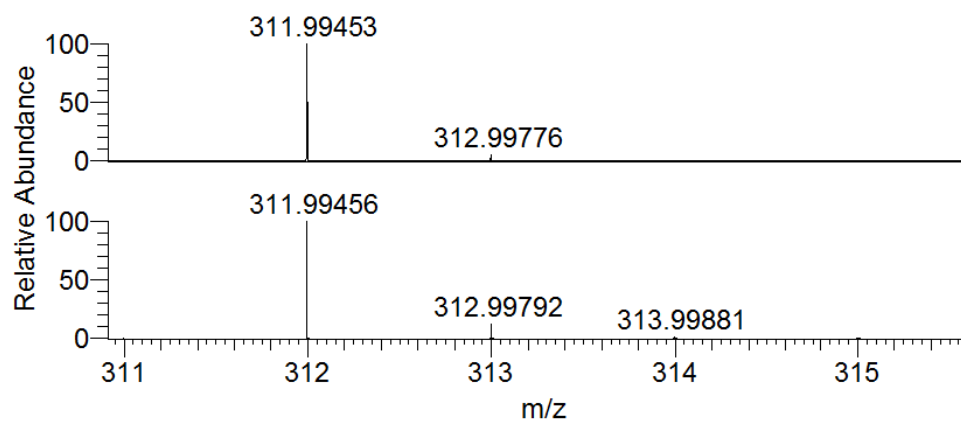
Ion	Composition	Experimental m/z <sup>a</sup>	Calculated m/z <sup>a</sup>	Error (ppm) <sup>b</sup>
$[Hacac+H]^+$	$C_5H_9O_2$	101.06019	101.05971	-4.7
$[Hacac+Na]^+$	$C_5H_8O_2Na$	123.04197	123.04165	-2.6
$[V^{IV}O(acac)_2+H]^+$	$C_{10}H_{15}O_5V$	266.03553	266.03536	-0.6
$[V^{IV}O(acac)_2+Na]^+$	$C_{10}H_{14}O_5VNa$	288.01750	288.01731	-0.7

<sup>a</sup> Experimental and calculated m/z values refer to the peak representative of the monoisotopic mass.

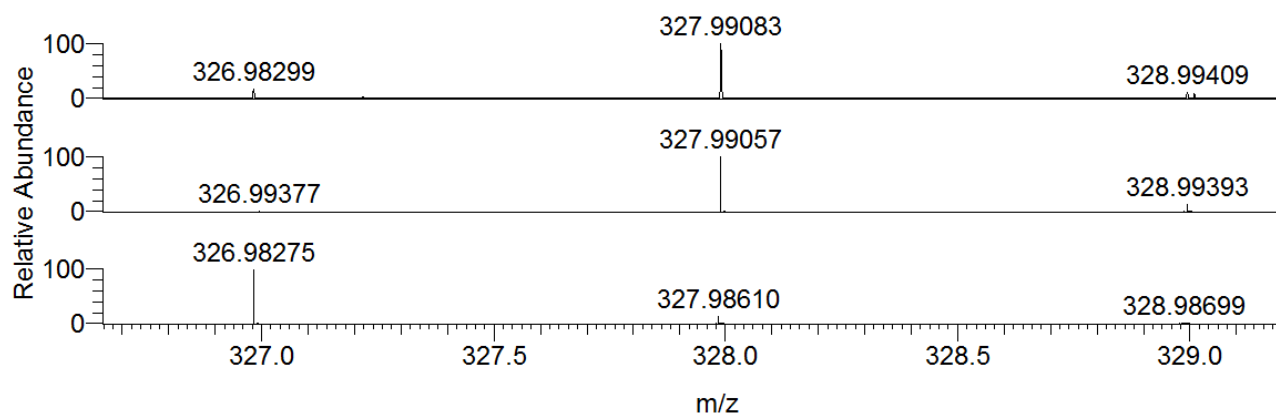
<sup>b</sup> Error in ppm respect to the experimental value, calculated as:  $10^6 \times \{[| \text{Calculated (m/z)} - \text{Experimental (m/z)} |] / \text{Calculated (m/z)}\}$ .



**Figure S1.** ESI-MS spectrum recorded in positive mode at pH 5.15 on the system containing  $[V^{IV}O(pic)_2(H_2O)]$  in ultrapure LC-MS water with a V concentration of 5  $\mu M$ .

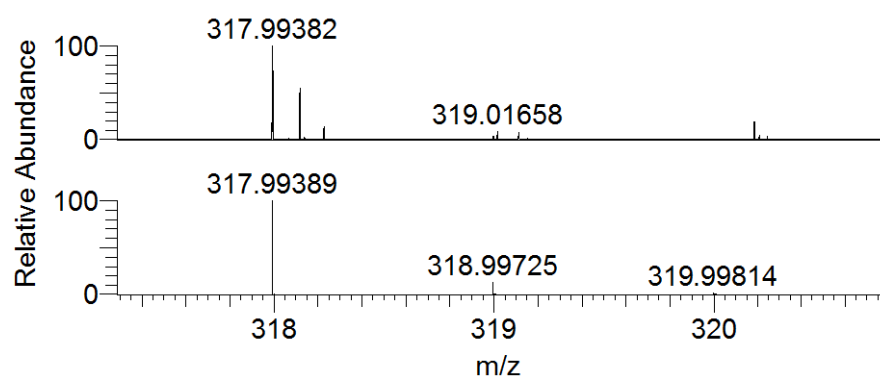


**Figure S2.** Experimental (top) and calculated (bottom) isotopic pattern of the species  $[V^{IV}O(pic)_2+H]^+$  ( $m/z = 311.99$ ).

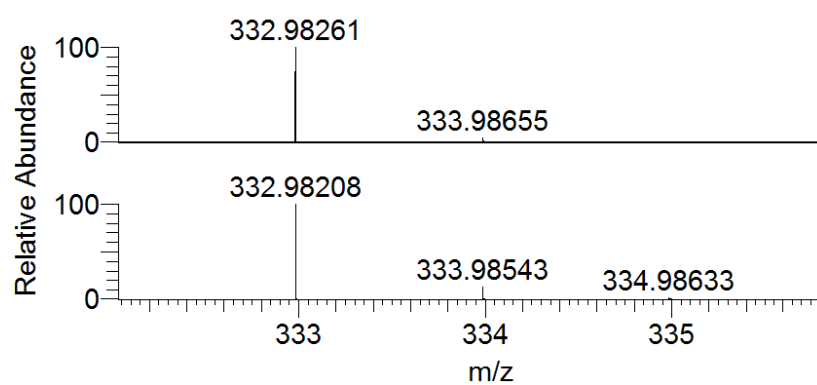


**Figure S3.** Experimental (top) and calculated isotopic pattern of  $[V^{IV}O(pic)_2(OH)]^-$  (centre) and  $[V^VO_2(pic)_2]^-$  (bottom).  $m/z = 327.99$  for  $[V^{IV}O(pic)_2(OH)]^-$  and  $m/z = 326.98$  for  $[V^VO_2(pic)_2]^-$ .

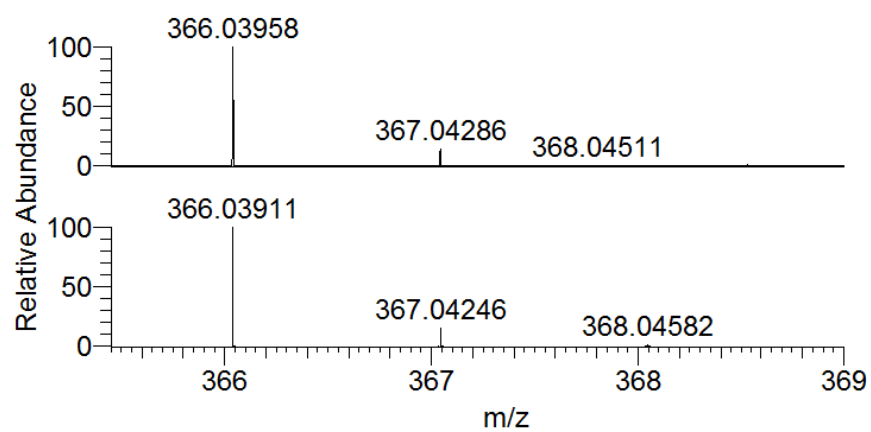




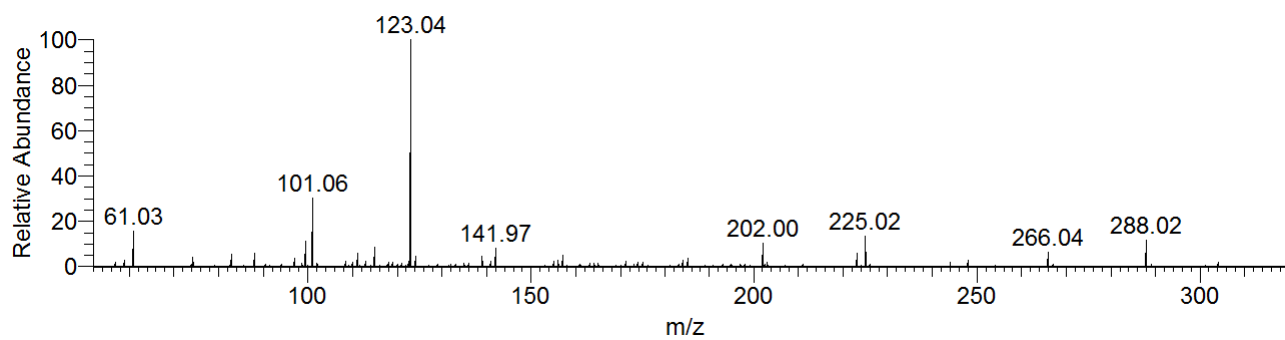
**Figure S4.** Experimental (top) and calculated (bottom) isotopic pattern of the species  $[V^{IV}O(ma)_2+H]^+$  ( $m/z = 317.99$ ).



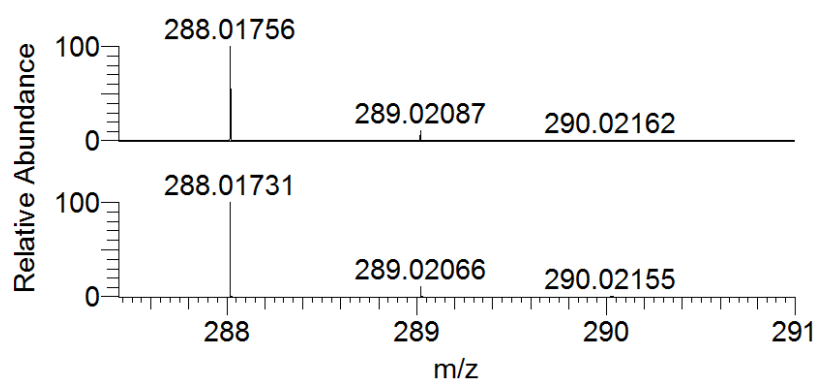
**Figure S5.** Experimental (top) and calculated (bottom) isotopic pattern of the species  $[V^VO_2(ma)_2]^-$  ( $m/z = 332.98$ ).



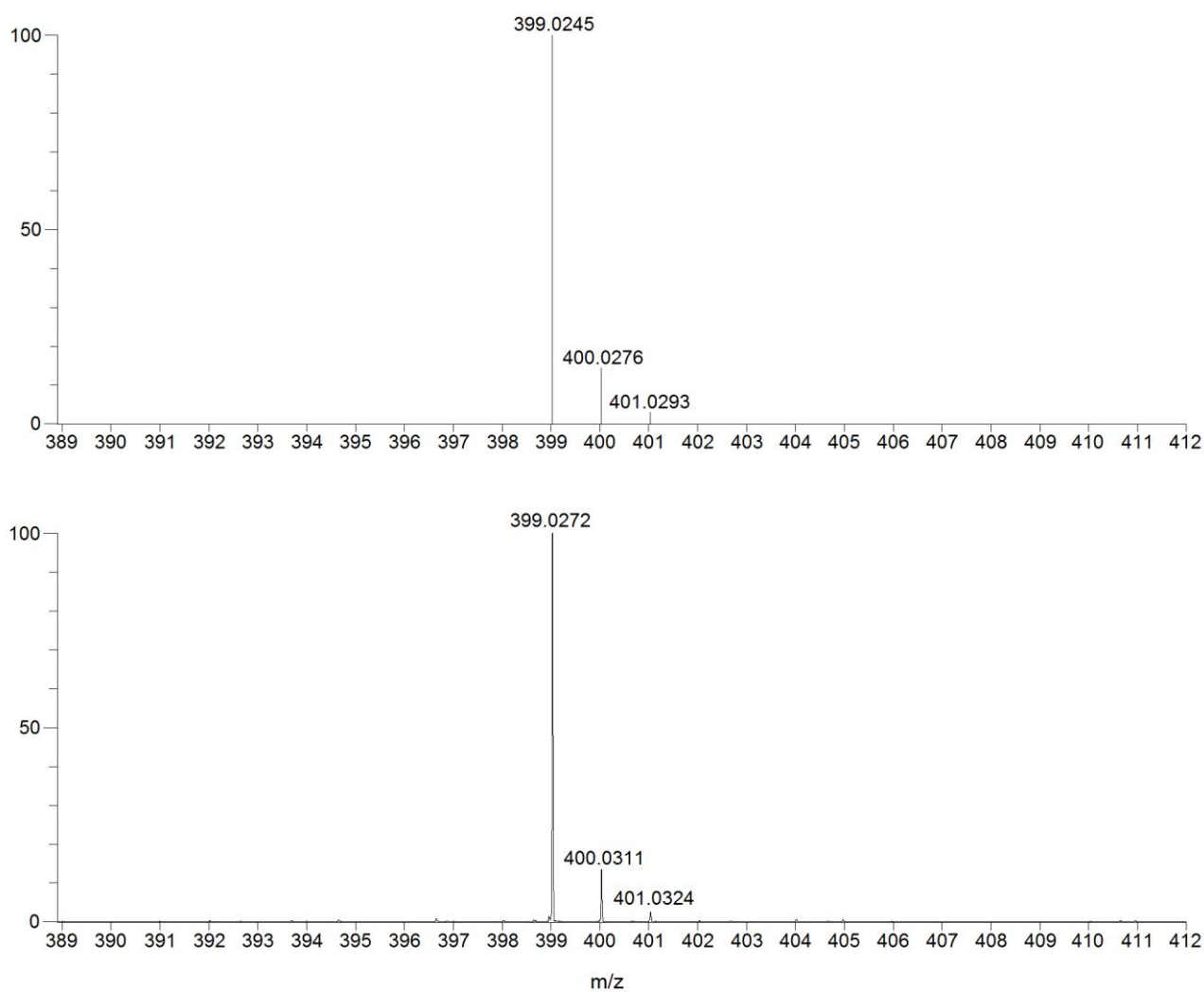
**Figure S6.** Experimental (top) and calculated (bottom) isotopic pattern of the species  $[V^{IV}O(dhp)_2+Na]^+$  ( $m/z = 366.04$ ).



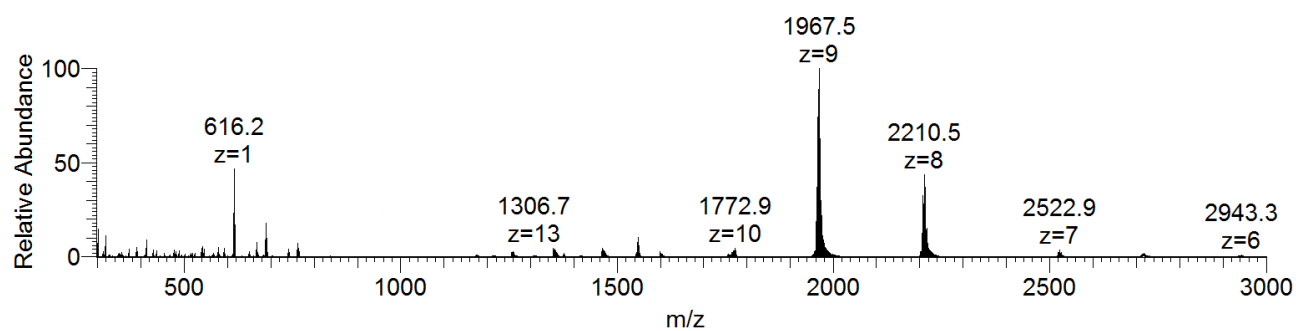
**Figure S7.** ESI-MS spectrum recorded in positive mode at pH 5.50 on the system containing [V<sup>IV</sup>O(acac)<sub>2</sub>] in ultrapure LC-MS water with a V concentration of 5.0  $\mu$ M.



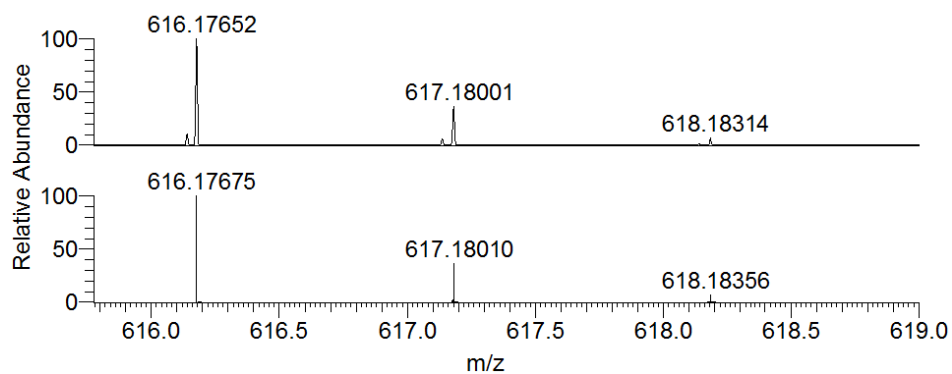
**Figure S8.** Experimental (top) and calculated (bottom) isotopic pattern of the species  $[V^{IV}O(acac)_2+Na]^+$  ( $m/z = 288.02$ ).



**Figure S9.** Experimental (top) and calculated (bottom) isotopic pattern of the species  $[V^V(hidpa)_2]^-$  ( $m/z = 399.02$ ).

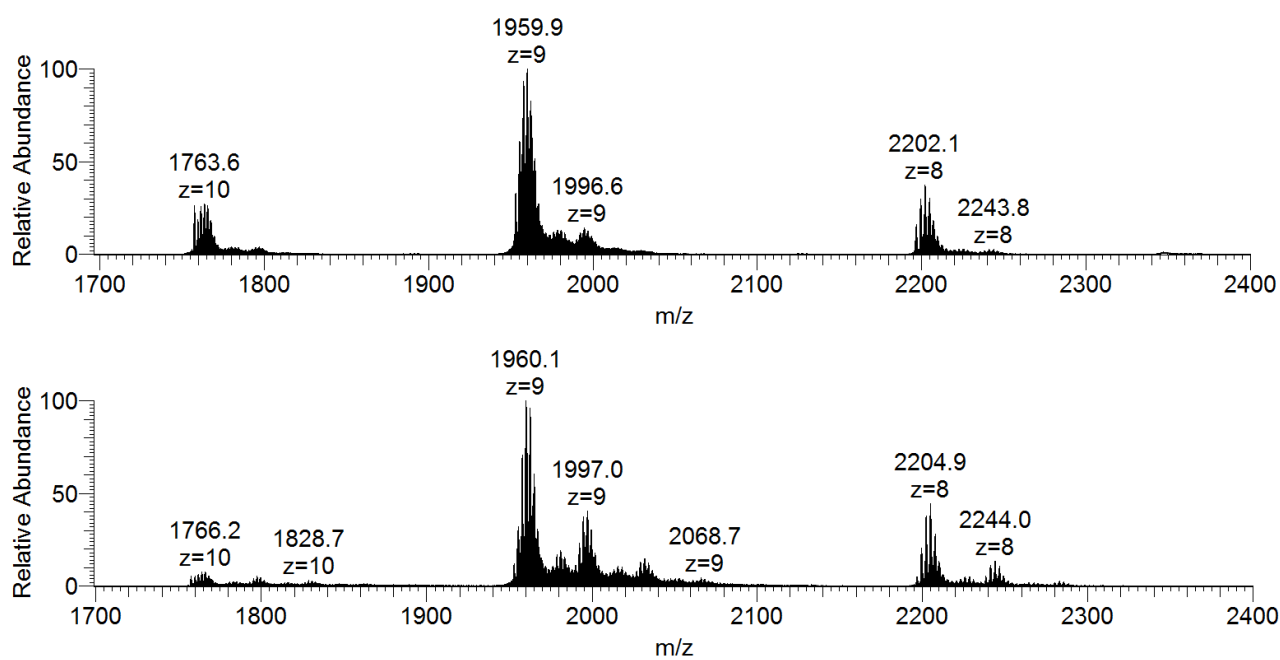


**Figure S10.** ESI-MS spectrum of myoglobin (concentration 5  $\mu$ M).

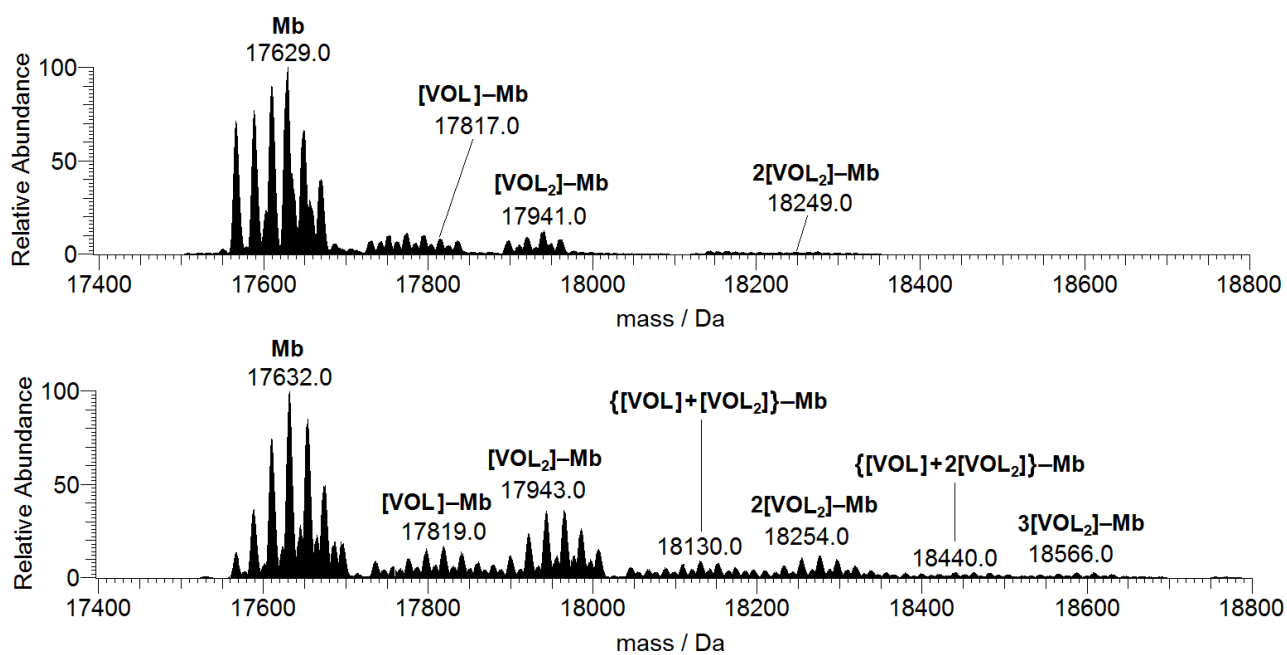


**Figure S11.** Experimental (top) and calculated (bottom) isotopic pattern for the peak of  $[\text{Fe}^{\text{III}}\text{heme}]^+$  group ( $\text{C}_{34}\text{H}_{32}\text{FeN}_4\text{O}_4$ ) revealed at  $m/z = 616.18$  in the ESI-MS spectrum of myoglobin (concentration  $5 \mu\text{M}$ ).

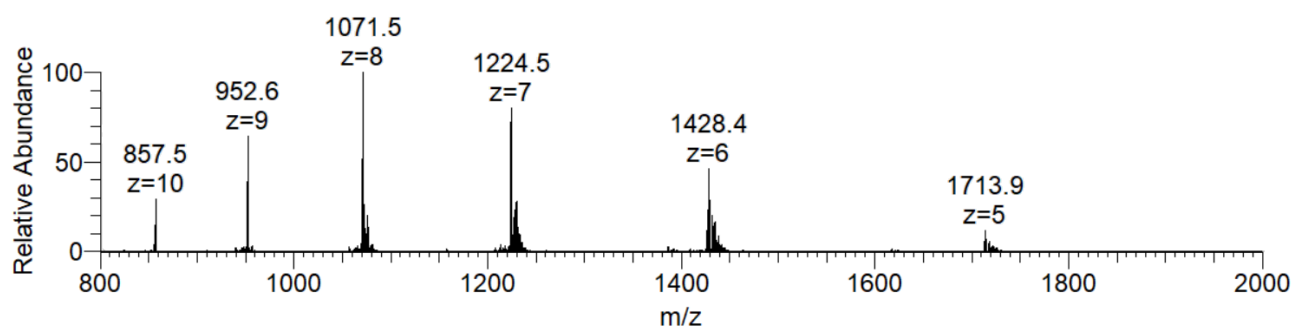




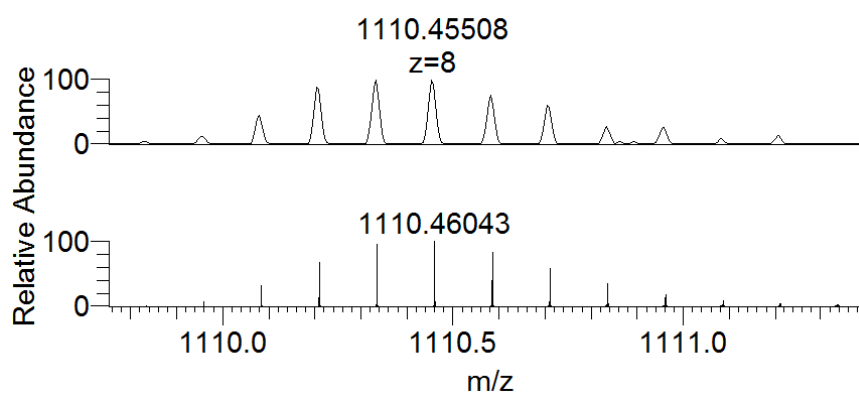
**Figure S12.** ESI-MS spectra recorded on the system containing  $[\text{V}^{\text{IV}}\text{O}(\text{pic})_2(\text{H}_2\text{O})]$  and myoglobin (5  $\mu\text{M}$ ): molar ratio 3/1 (top) and 5/1 (bottom).



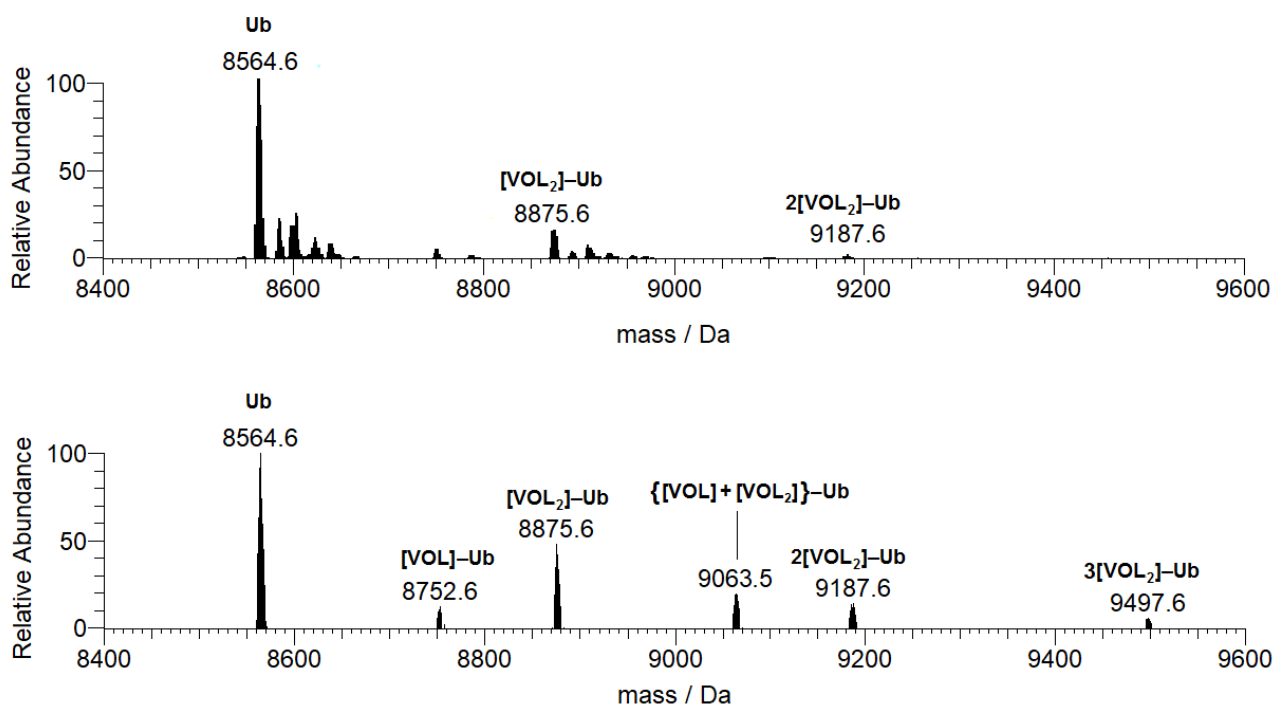
**Figure S13.** Deconvoluted ESI-MS spectra recorded on the system containing  $[\text{V}^{\text{IV}}\text{O}(\text{pic})_2(\text{H}_2\text{O})]$  and myoglobin (5  $\mu\text{M}$ ): molar ratio 3/1 (top) and 5/1 (bottom). L indicates the picolinato ligand.



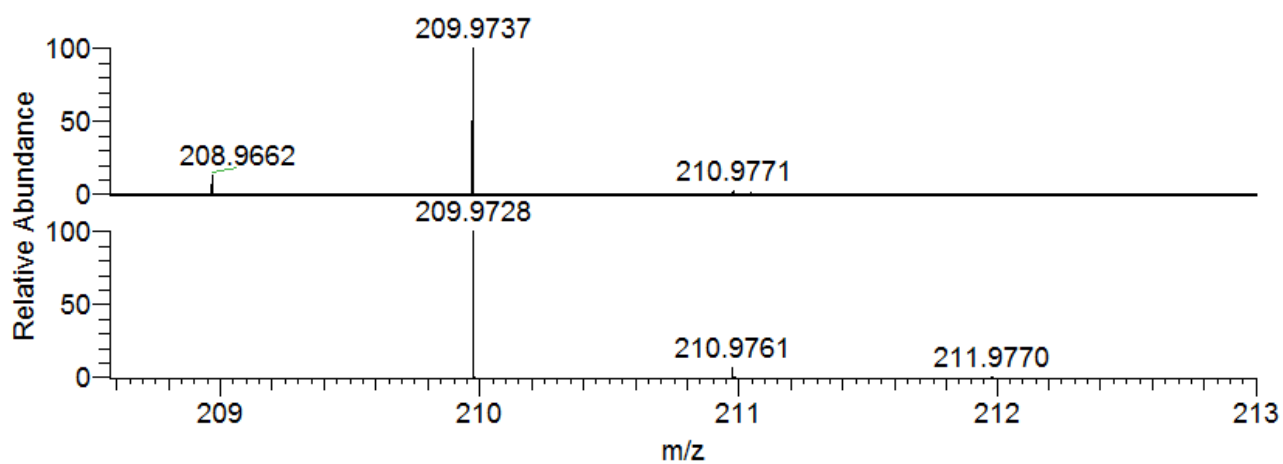
**Figure S14.** ESI-MS spectrum of ubiquitin (concentration 5  $\mu$ M).



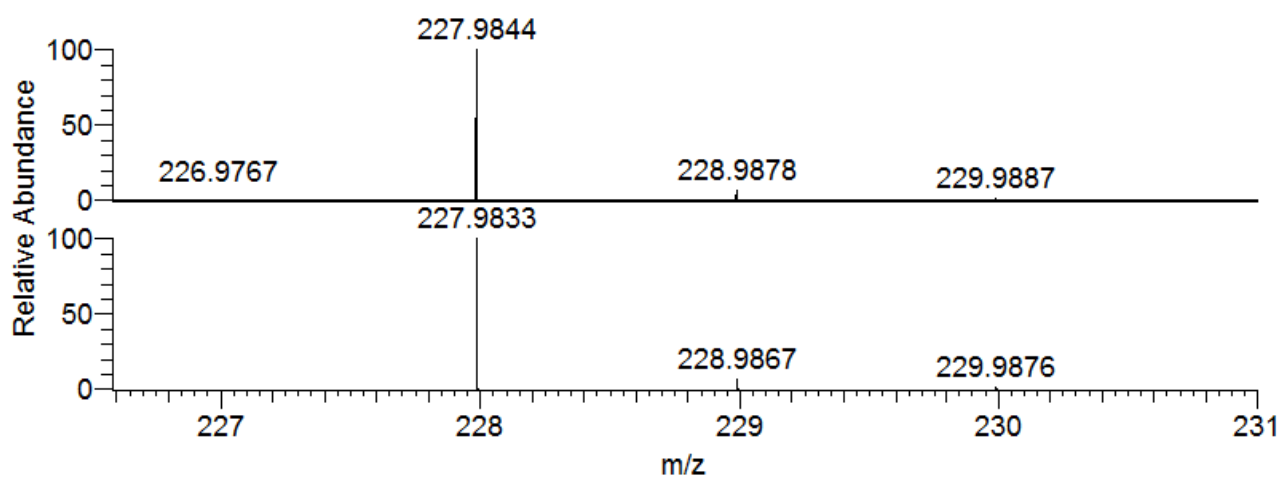
**Figure S15.** Experimental (top) and calculated (bottom) isotopic pattern for the peak of  $[\text{V}^{\text{IV}}\text{O}(\text{pic})_2]\text{-Ub}$  ( $m/z = 1110.46$ ,  $z = 8$ ) with formula  $\text{C}_{390}\text{H}_{638}\text{N}_{107}\text{O}_{123}\text{SV}$  detected in the ESI-MS spectrum of the system containing  $[\text{V}^{\text{IV}}\text{O}(\text{pic})_2(\text{H}_2\text{O})]$  and ubiquitin with ratio 3/1 and Ub concentration of 5  $\mu\text{M}$ .



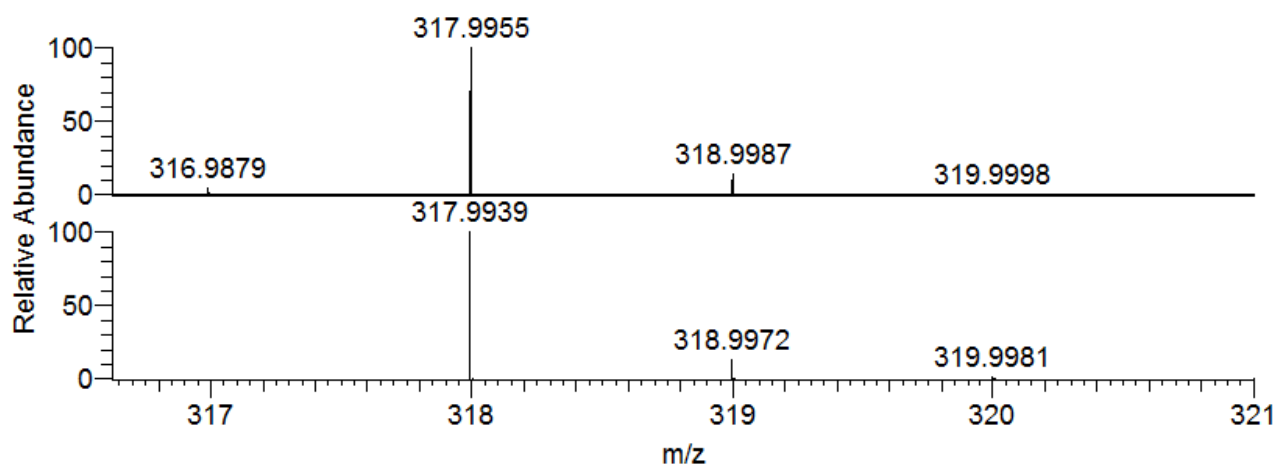
**Figure S16.** Deconvoluted ESI-MS spectra recorded on the system containing  $[V^{IV}O(pic)_2(H_2O)]$  and ubiquitin (50  $\mu M$ ): molar ratio 3/1 (top) and 5/1 (bottom). L indicates the picolinato ligand.



**Figure S17.** Experimental (top) and calculated (bottom) isotopic pattern of  $[V^{IV}O(ma)(H_2O)]^+$  detected in the ESI-MS spectrum of the system containing  $[V^{IV}O(ma)_2]$  (150  $\mu$ M) and lysozyme (50  $\mu$ M) ( $m/z = 209.97$ ).

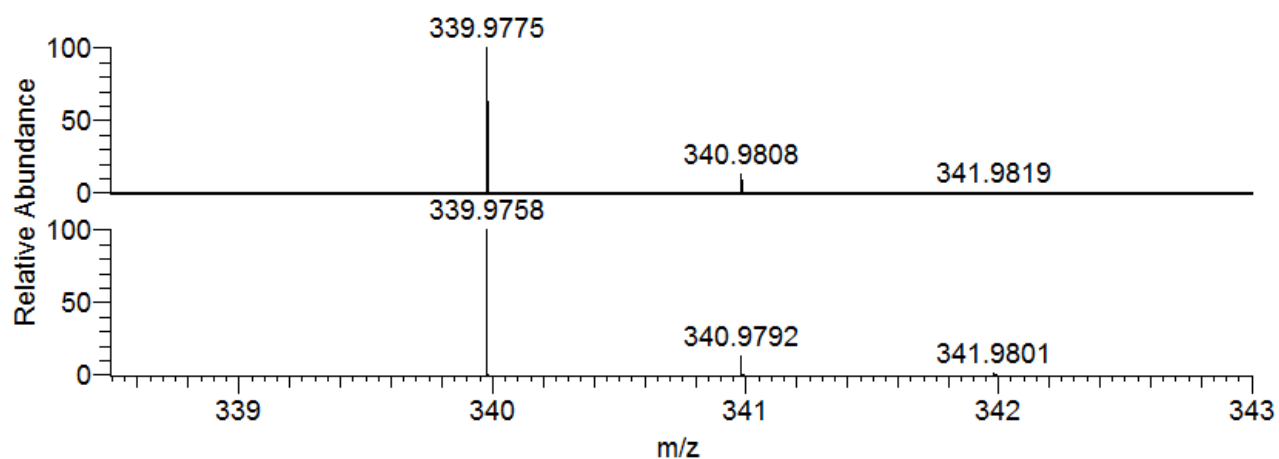


**Figure S18.** Experimental (top) and calculated (bottom) isotopic pattern of  $[\text{V}^{\text{IV}}\text{O}(\text{ma})(\text{H}_2\text{O})_2]^+$  detected in the ESI-MS spectrum of the system containing  $[\text{V}^{\text{IV}}\text{O}(\text{ma})_2]$  (150  $\mu\text{M}$ ) and lysozyme (50  $\mu\text{M}$ ) ( $m/z = 227.98$ ).

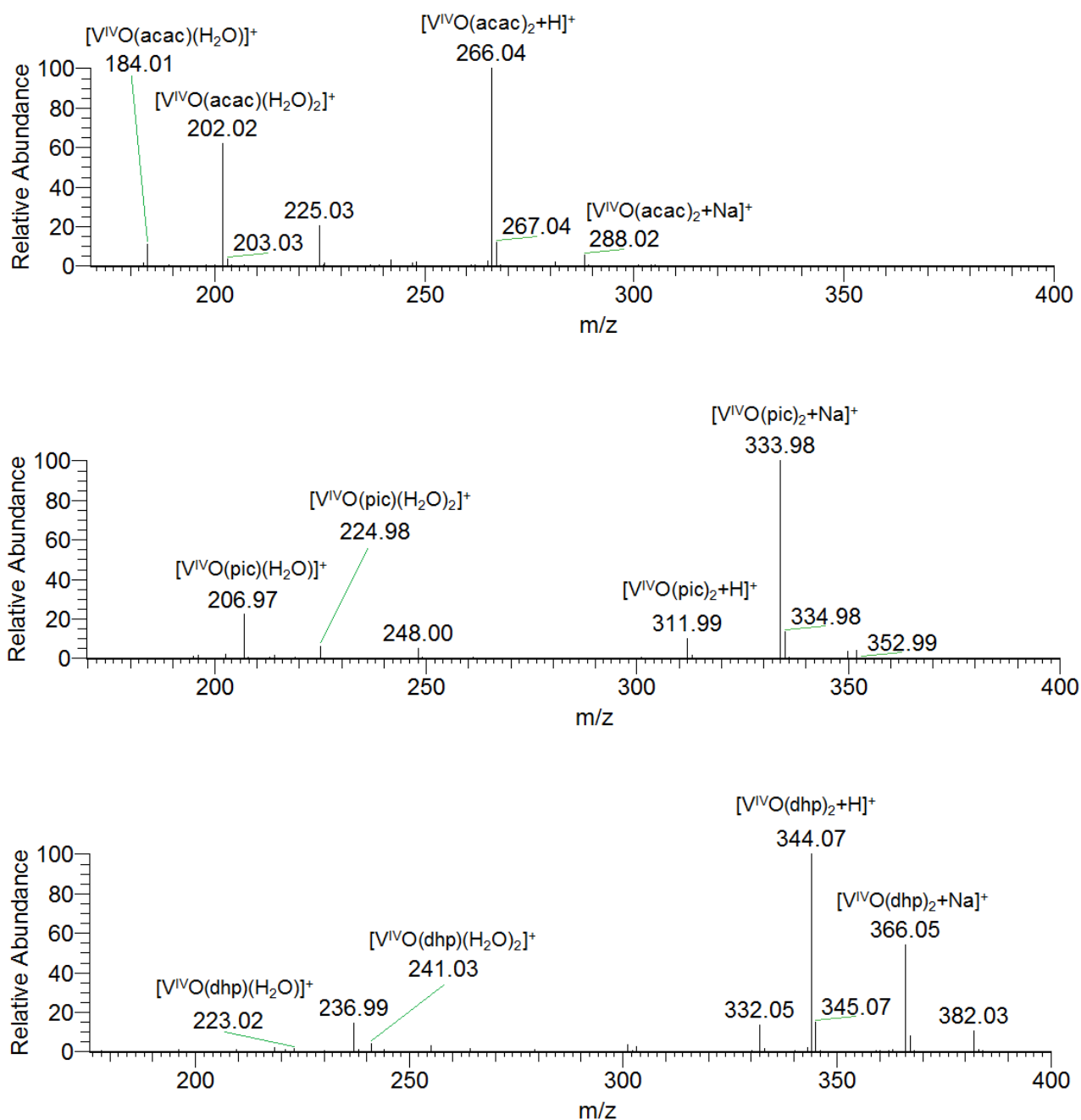


**Figure S19.** Experimental (top) and calculated (bottom) isotopic pattern of  $[\text{V}^{\text{IV}}\text{O}(\text{ma})_2\text{H}]^+$ , detected in the ESI-MS spectrum of the system containing  $[\text{V}^{\text{IV}}\text{O}(\text{ma})_2]$  (150  $\mu\text{M}$ ) and lysozyme (50  $\mu\text{M}$ ) ( $m/z = 318.00$ ).

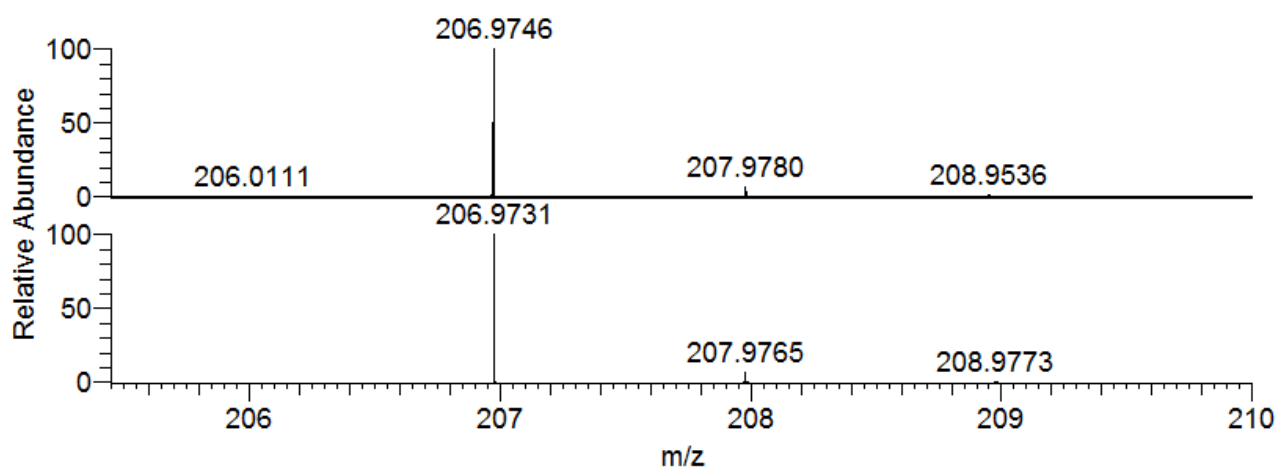




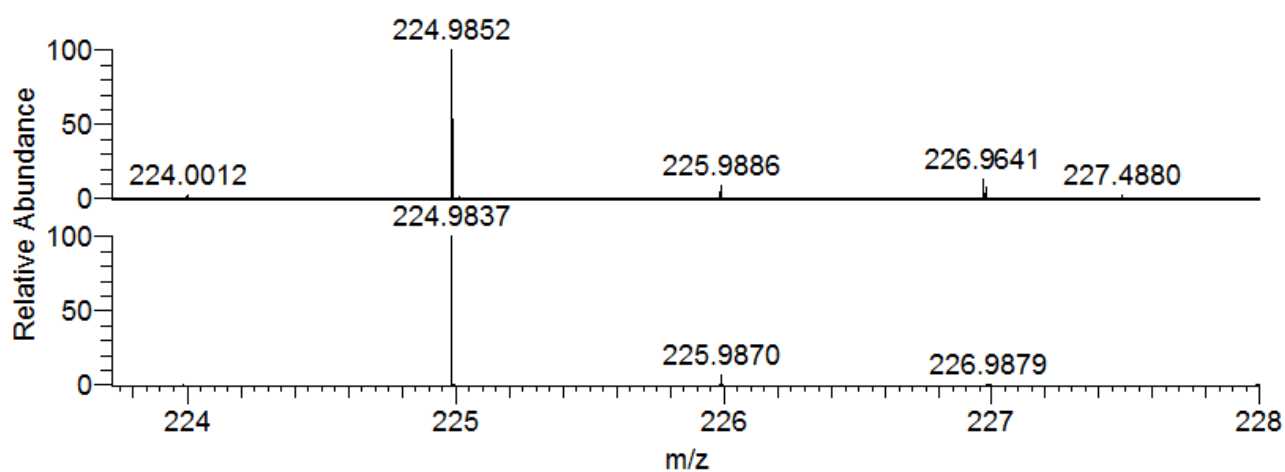
**Figure S20.** Experimental (top) and calculated (bottom) isotopic pattern of  $[V^{IV}O(ma)_2+Na]^+$  detected in the ESI-MS spectrum of the system containing  $[V^{IV}O(ma)_2]$  (150  $\mu$ M) and lysozyme (50  $\mu$ M) ( $m/z$  = 339.98).



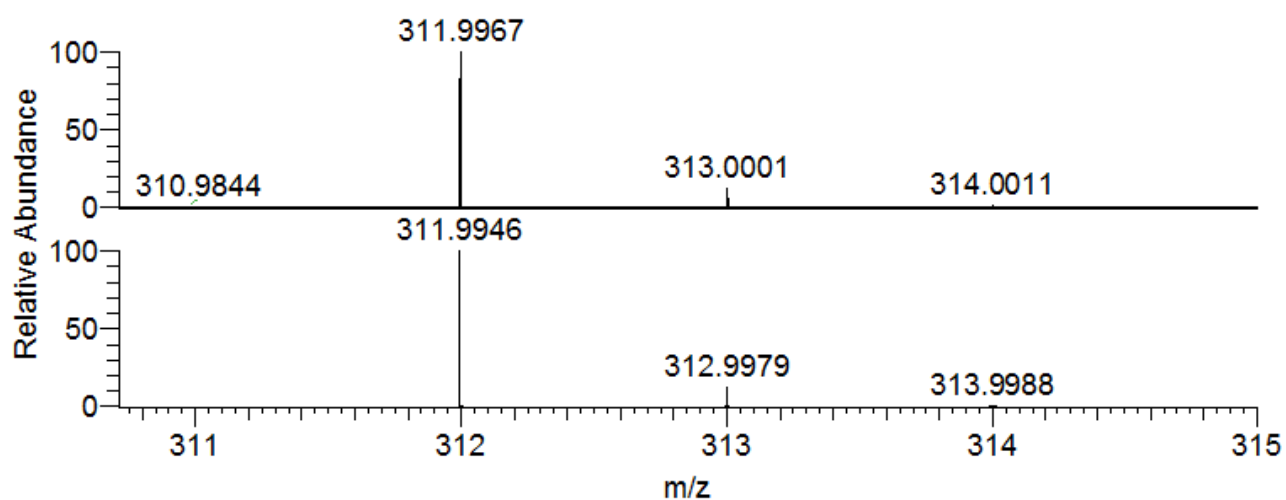
**Figure S21.** Region in the m/z range 180-400 of the ESI-MS spectra recorded on the systems containing  $[V^{IV}O(acac)_2]$  (150  $\mu$ M) and lysozyme (50  $\mu$ M) (top),  $[V^{IV}O(pic)_2(H_2O)_2]$  (150  $\mu$ M) and lysozyme (50  $\mu$ M) (centre), and  $[V^{IV}O(dhp)_2]$  (150  $\mu$ M) and lysozyme (50  $\mu$ M) (bottom).



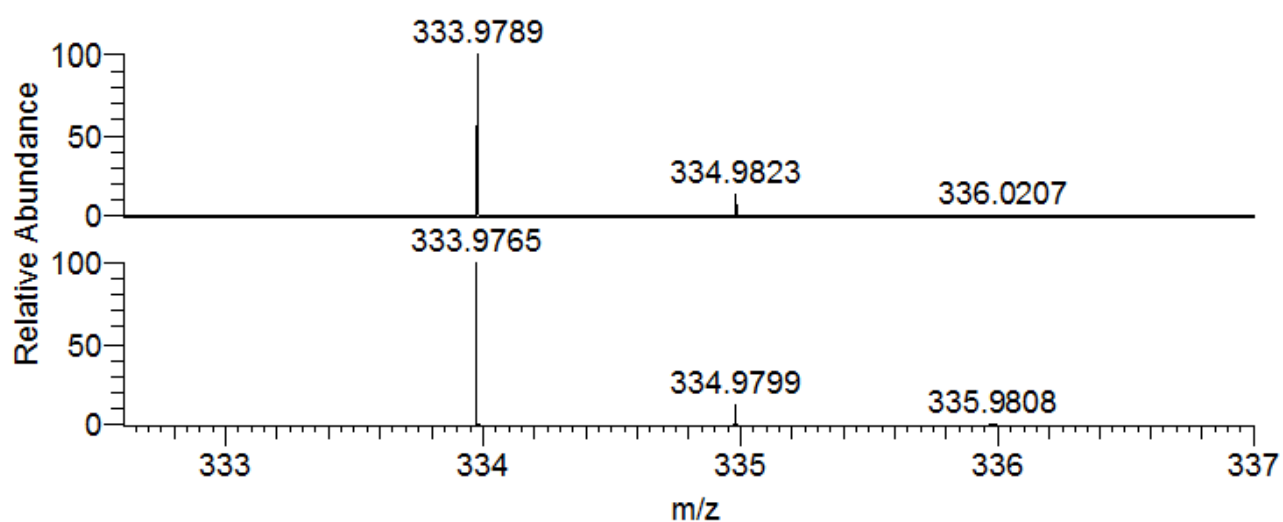
**Figure S22.** Experimental (top) and calculated (bottom) isotopic pattern of  $[V^{IV}O(pic)(H_2O)]^+$  detected in the ESI-MS spectrum of the system containing  $[V^{IV}O(pic)_2(H_2O)]$  (150  $\mu$ M) and lysozyme (50  $\mu$ M) ( $m/z$  = 206.97).



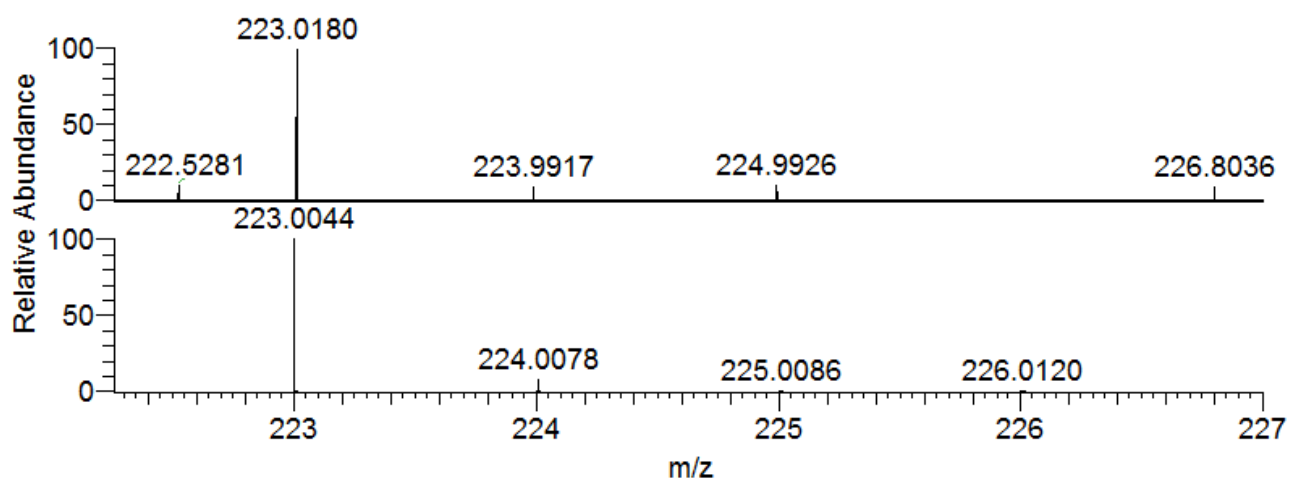
**Figure S23.** Experimental (top) and calculated (bottom) isotopic pattern of  $[\text{V}^{\text{IV}}\text{O}(\text{pic})(\text{H}_2\text{O})_2]^+$  detected in the ESI-MS spectrum of the system containing  $[\text{V}^{\text{IV}}\text{O}(\text{pic})_2(\text{H}_2\text{O})]$  (150  $\mu\text{M}$ ) and lysozyme (50  $\mu\text{M}$ ) ( $m/z = 224.99$ ).



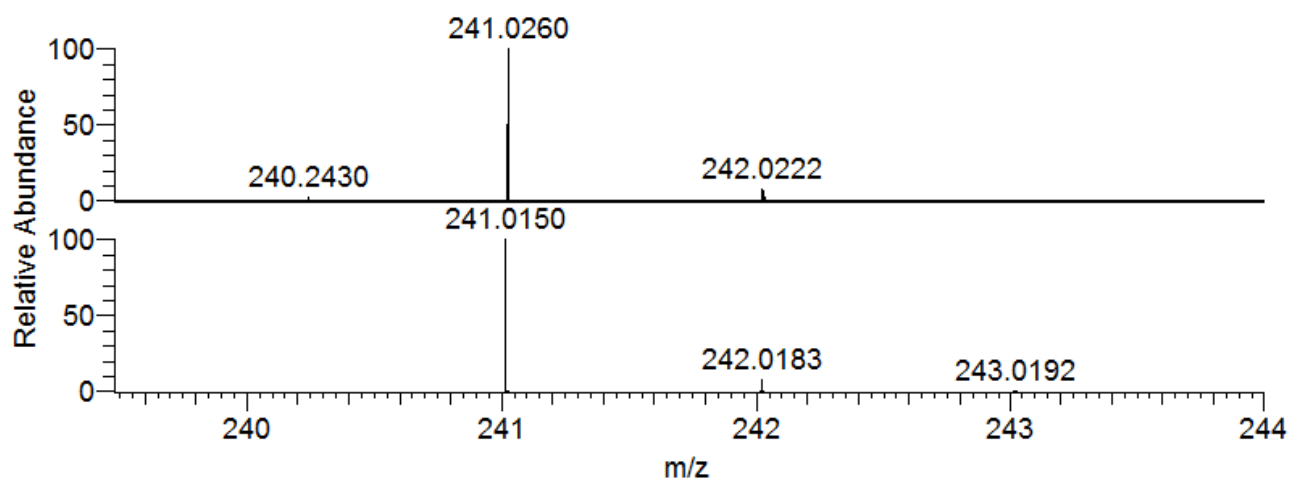
**Figure S24.** Experimental (top) and calculated (bottom) isotopic pattern of  $[\text{V}^{\text{IV}}\text{O}(\text{pic})_2+\text{H}]^+$ , detected in the ESI-MS spectrum of the system containing  $[\text{V}^{\text{IV}}\text{O}(\text{pic})_2(\text{H}_2\text{O})]$  (150  $\mu\text{M}$ ) and lysozyme (50  $\mu\text{M}$ ) ( $m/z = 312.00$ ).



**Figure S25.** Experimental (top) and calculated (bottom) isotopic pattern of  $[\text{V}^{\text{IV}}\text{O}(\text{pic})_2+\text{Na}]^+$ , detected in the ESI-MS spectrum of the system containing  $[\text{V}^{\text{IV}}\text{O}(\text{pic})_2(\text{H}_2\text{O})]$  (150  $\mu\text{M}$ ) and lysozyme (50  $\mu\text{M}$ ) ( $m/z = 333.98$ ).

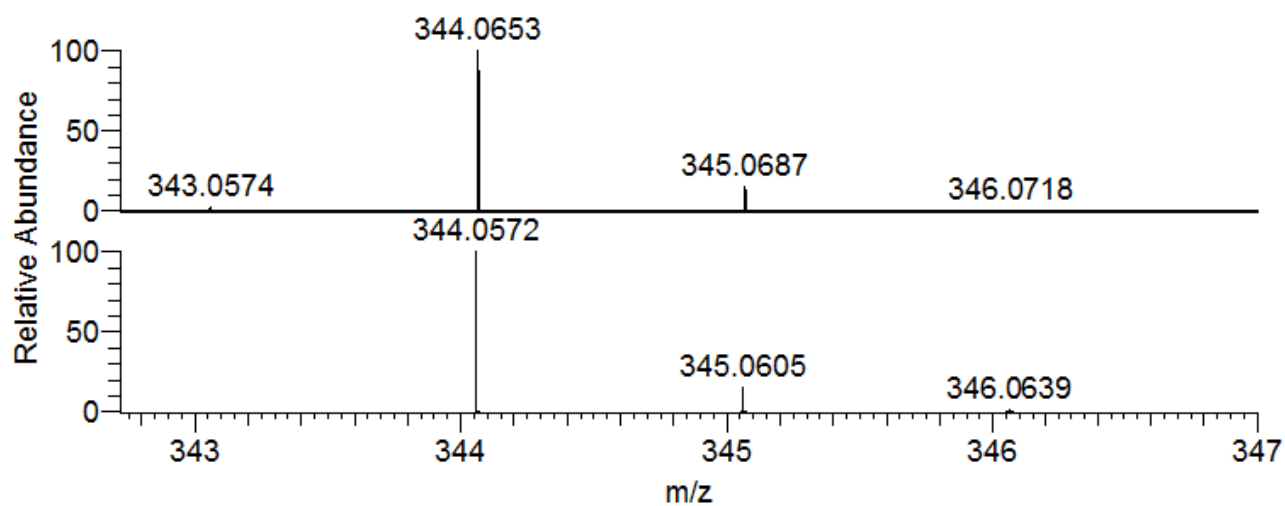


**Figure S26.** Experimental (top) and calculated (bottom) isotopic pattern of  $[V^{IV}O(dhp)(H_2O)]^+$  detected in the ESI-MS spectrum of the system containing  $[V^{IV}O(dhp)_2]$  (150  $\mu$ M) and lysozyme (50  $\mu$ M) ( $m/z$  = 223.02).

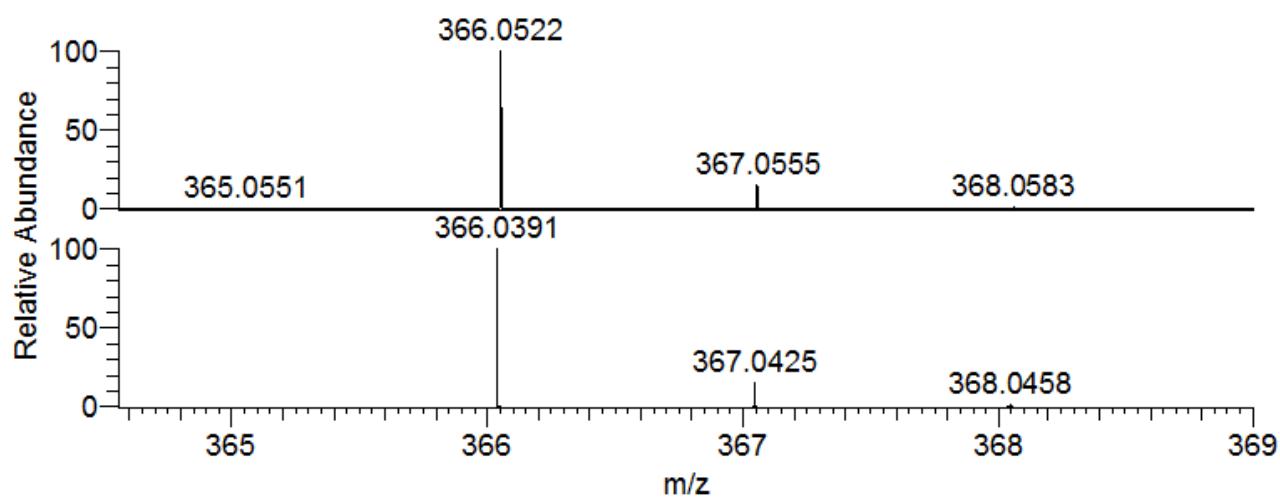


**Figure S27.** Experimental (top) and calculated (bottom) isotopic pattern of  $[\text{V}^{\text{IV}}\text{O}(\text{dhp})(\text{H}_2\text{O})_2]^+$  detected in the ESI-MS spectrum of the system containing  $[\text{V}^{\text{IV}}\text{O}(\text{dhp})_2]$  (150  $\mu\text{M}$ ) and lysozyme (50  $\mu\text{M}$ ) ( $m/z = 241.03$ ).

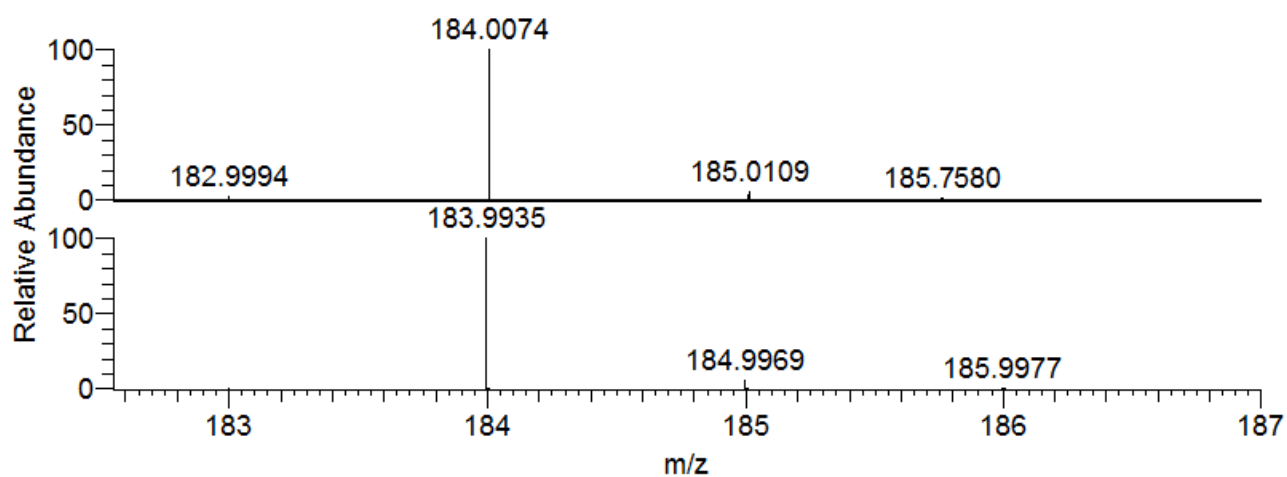




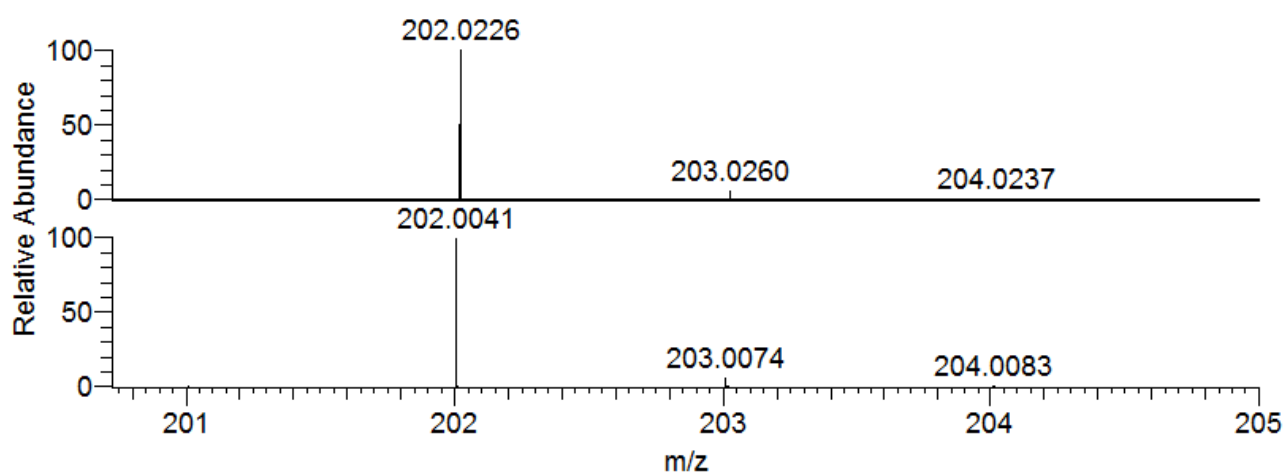
**Figure S28.** Experimental (top) and calculated (bottom) isotopic pattern of  $[\text{V}^{\text{IV}}\text{O}(\text{dhp})_2+\text{H}]^+$ , detected in the ESI-MS spectrum of the system containing  $[\text{V}^{\text{IV}}\text{O}(\text{dhp})_2]$  (150  $\mu\text{M}$ ) and lysozyme (50  $\mu\text{M}$ ) ( $m/z = 344.07$ ).



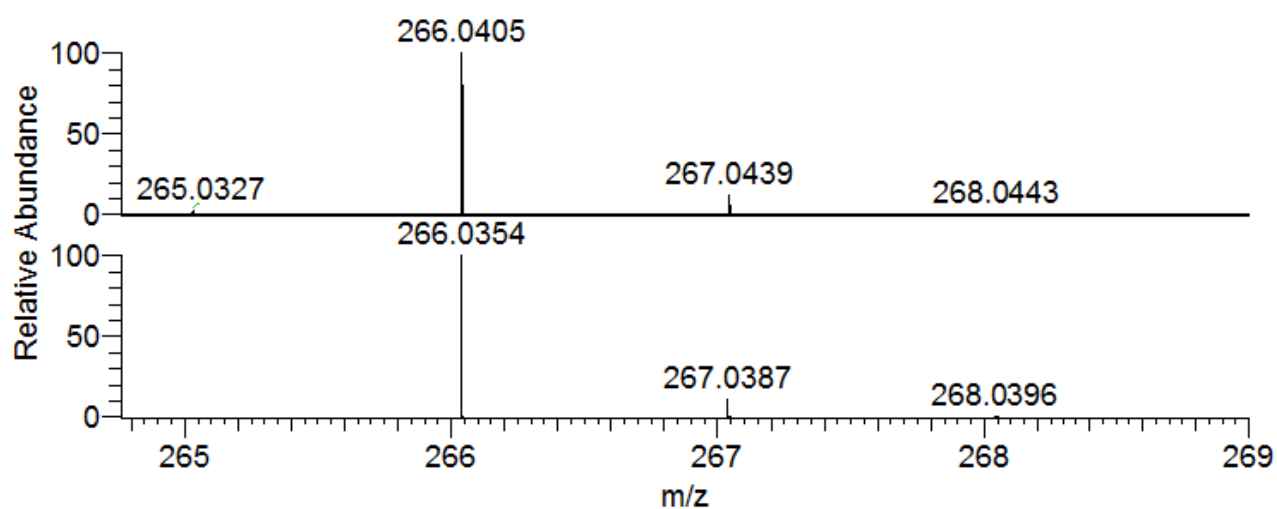
**Figure S29.** Experimental (top) and calculated (bottom) isotopic pattern of  $[\text{V}^{\text{IV}}\text{O}(\text{dhp})_2+\text{Na}]^+$ , detected in the ESI-MS spectrum of the system containing  $[\text{V}^{\text{IV}}\text{O}(\text{dhp})_2]$  (150  $\mu\text{M}$ ) and lysozyme (50  $\mu\text{M}$ ) ( $m/z = 366.05$ ).



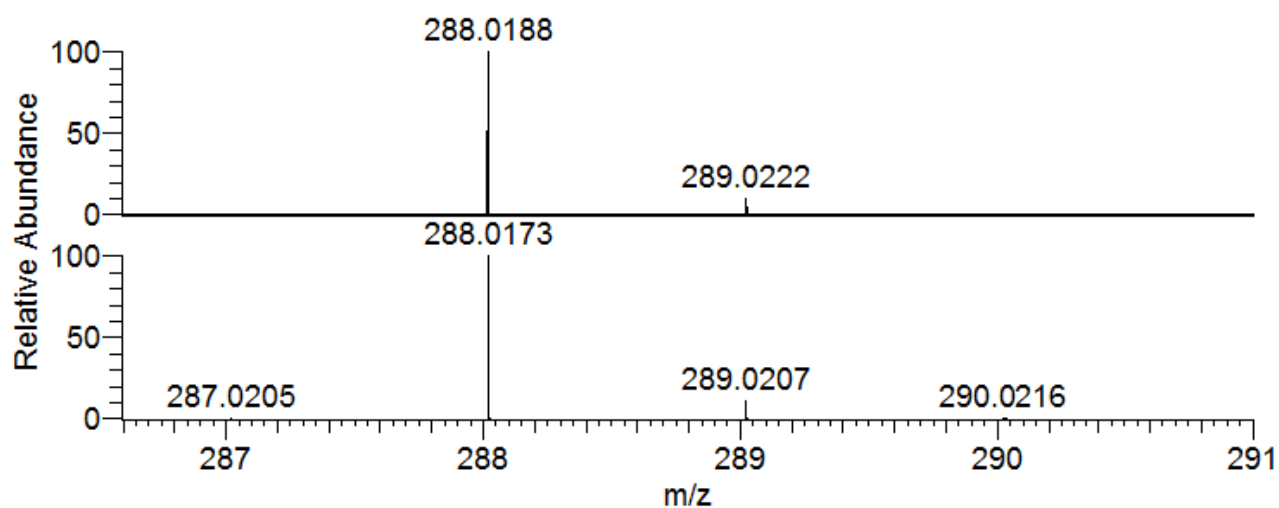
**Figure S30.** Experimental (top) and calculated (bottom) isotopic pattern of  $[\text{V}^{\text{IV}}\text{O}(\text{acac})(\text{H}_2\text{O})]^+$  detected in the ESI-MS spectrum of the system containing  $[\text{V}^{\text{IV}}\text{O}(\text{acac})_2]$  (150  $\mu\text{M}$ ) and lysozyme (50  $\mu\text{M}$ ) ( $m/z = 184.01$ ).



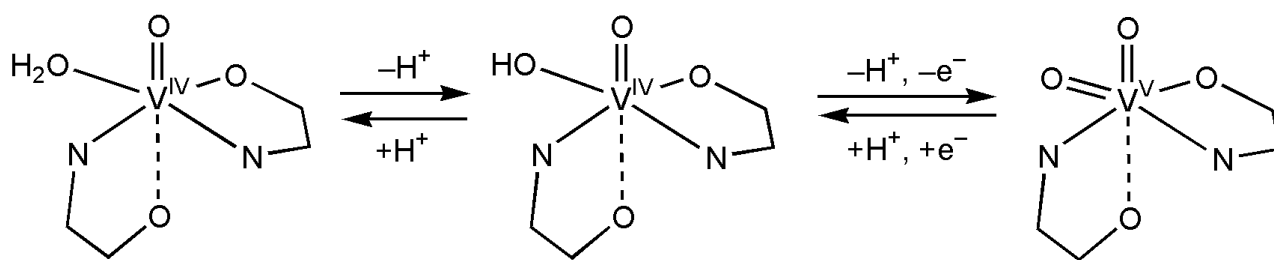
**Figure S31.** Experimental (top) and calculated (bottom) isotopic pattern of  $[\text{V}^{\text{IV}}\text{O}(\text{acac})(\text{H}_2\text{O})_2]^+$  detected in the ESI-MS spectrum of the system containing  $[\text{V}^{\text{IV}}\text{O}(\text{acac})_2]$  (150  $\mu\text{M}$ ) and lysozyme (50  $\mu\text{M}$ ) ( $m/z = 202.02$ ).



**Figure S32.** Experimental (top) and calculated (bottom) isotopic pattern of  $[\text{V}^{\text{IV}}\text{O}(\text{acac})_2 + \text{H}]^+$  detected in the ESI-MS spectrum of the system containing  $[\text{V}^{\text{IV}}\text{O}(\text{acac})_2]$  (150  $\mu\text{M}$ ) and lysozyme (50  $\mu\text{M}$ ) ( $m/z = 266.04$ ).



**Figure S33.** Experimental (top) and calculated (bottom) isotopic pattern of  $[\text{V}^{\text{IV}}\text{O}(\text{acac})_2 + \text{Na}]^+$  detected in the ESI-MS spectrum of the system containing  $[\text{V}^{\text{IV}}\text{O}(\text{acac})_2]$  (150  $\mu\text{M}$ ) and lysozyme (50  $\mu\text{M}$ ) ( $m/z = 288.02$ ).



**Scheme S1.** Oxidation of *cis*-V<sup>IV</sup>O(H<sub>2</sub>O)<sup>2+</sup> to *cis*-V<sup>V</sup>O<sub>2</sub><sup>+</sup> moiety.